

17. Yatsun, V., Filimonikhin, G., Dumenko, K., Nevdakha, A. (2017). Equations of motion of vibration machines with a translational motion of platforms and a vibration exciter in the form of a passive auto-balancer. Eastern-European Journal of Enterprise Technologies, 5 (1 (89)), 19–25. doi: <https://doi.org/10.15587/1729-4061.2017.111216>
18. Yatsun, V., Filimonikhin, G., Dumenko, K., Nevdakha, A. (2018). Search for the dualfrequency motion modes of a dualmass vibratory machine with a vibration exciter in the form of passive autobalancer. Eastern-European Journal of Enterprise Technologies, 1 (7 (91)), 47–54. doi: <https://doi.org/10.15587/1729-4061.2018.121737>
19. Yatsun, V., Filimonikhin, G., Podoprygora, N., Pirogov, V. (2019). Studying the excitation of resonance oscillations in a rotor on isotropic supports by a pendulum, a ball, a roller. Eastern-European Journal of Enterprise Technologies, 6 (7 (102)), 32–43. doi: <https://doi.org/10.15587/1729-4061.2019.182995>
20. Filimonikhin, G., Yatsun, V., Filimonikhina, I. (2020). Investigation of oscillations of platform on isotropic supports excited by a pendulum. E3S Web of Conferences, 168, 00025. doi: <https://doi.org/10.1051/e3sconf/202016800025>

*Метою дослідження є обґрунтування умов стійкості відкатних штреків при розробці крутих вугільних пластів.*

*В процесі моделювання стійкості штреків встановлено, що напружено-деформований стан бічних порід в вуглепородному масиві дільниці покрівлі, який вміщає виробки, залежить від фізико-механічних властивостей покрівлі і ґрунту вугільного пласта, що розробляється, жорсткості охоронних споруд і довжини підтримуваної охоронною спорудою. Зі збільшенням довжини, яка підтримується охоронною спорудою дільниці покрівлі, при мінімальній жорсткості піддатливих опор, збільшується зона плавного прогину бічних порід над відкатним штреком і знижується рівень їх напружено-деформованого стану.*

*Доведено, що при підтримці гірничих виробок в глибоких шахтах зниження напружено-деформованого стану бічних порід при застосуванні закладки виробленого простору відбувається в результаті ущільнення закладного масиву, на який стираються породи покрівлі, коли значення коефіцієнта ущільнення вихідного матеріалу приймають максимальні значення, що дорівнюють  $k_{\text{ущ}} = 1.5 - 1.53$ . При використанні штучних піддатливих охоронних споруд, що зводяться над штреком, зміна напружено-деформованого стану відбувається в результаті стиснення опор, коли переміщення порід покрівлі і ґрунту обмежуються, а площа контакту бічних порід з засобами охорони збільшується.*

*При виборі способу охорони відкатних штреків необхідно враховувати параметри охоронних споруд, тому що вплив розмірів одних і тих же опор, при однаковій жорсткості на розподіл напружень в вуглепородному масиві, різноманітний.*

*Для забезпечення експлуатаційного стану дільничних підготовчих виробок, при розробці крутих вугільних пластів, доцільно застосування піддатливих охоронних споруд, розташованих над відкатним штреком, які обмежують переміщення бічних порід у виробленому просторі*

*Ключові слова: гірський тиск, очисний вибій, обвалення бічних порід, закладка виробленого простору, піддатливі опори*

UDC 622.268.6:622.834

DOI: 10.15587/1729-4061.2020.202483

# SUBSTANTIATION OF THE STABILITY OF HAULAGE DRIFTS WITH PROTECTIVE STRUCTURES OF DIFFERENT RIGIDITY

I. Iordanov

PhD, Chairman of the Board  
LLC "MC ELTEKO"

Tykoho str., 3, Kostiantynivka, Ukraine, 85103

Yu. Simonova

Postgraduate Student\*

E-mail: yuliia.simonova@donntu.edu.ua

O. Kayun

Postgraduate Student\*

Ye. Podkopayev

Postgraduate Student\*

A. Polozhii

Postgraduate Student\*

H. Boichenko

Director

"SVYATO-POKROVSKAYA No. 3 MINE" LLC  
Shybankova sq., 1a, Pokrovsk, Ukraine, 85300

\*Department of Mining of Mineral Deposits

Donetsk National Technical University

Shybankova sq., 2, Pokrovsk, Ukraine, 85300

Received date 18.02.2020

Accepted date 11.05.2020

Published date 19.06.2020

Copyright © 2020, I. Iordanov, Yu. Simonova, O. Kayun, Ye. Podkopayev, A. Polozhii, H. Boichenko

This is an open access article under the CC BY license

<http://creativecommons.org/licenses/by/4.0>

## 1. Introduction

The coal industry is the main supplier of high-quality coal for the steel industry and energy. According to experts [1], the possible depth of development of high-quality coking

coal, under conditions of steep coal seams, is 1,700 m, with balance reserves reaching 1.14 billion tons.

Despite that, at present, the development of steep high-quality coal seams is characterized by a relatively low level of the technical and economic indicators. In no small

part, this is due to the lack of reliable and effective ways to protect haulage drifts.

The current protection techniques of preparatory workings do not provide reliable protection of haulage drifts from harmful manifestations of mountain pressure, which requires a large amount of repair work, which does not lend itself to mechanization. Therefore, the search for more reliable ways to protect haulage drifts is one of the main areas of increasing the efficiency of the development of steep coal seams under difficult conditions of great depths, which, therefore, confirms the relevance of our research to substantiate the stability of section preparatory workings.

---

## 2. Literature review and problem statement

---

The world experience of deep mine operation shows that the efficiency of coal seam development depends on the stability of side rocks and the state of mining workings. Paper [2] reports the results of a study into the manifestations of mountain pressure in haulage drifts at the different protection techniques. It is shown that in a coal-rock massif, in the unloading zones, clay rocks, while increasing in volume, contribute to the stratification of side rocks and form the conditions of their collapses. However, nothing is said about the prevention of side rock stratifications and collapses of the roof of the worked coal seam, which lead to the collapsing of the exploited haulage drifts.

Taking into consideration the properties of a coal-rock massif that accommodates the workings, study [3] addresses the features of interaction of the stratified roof at the hinge-block movement of side rocks over the worked space. When clarifying the mechanism of displacement of stratified rocks, in the vicinity of the maintained mining workings, the study has no recommendations on the effective support of the roof and soil of the coal seam behind the breakage face, which negatively affects the stability of haulage drifts.

The use of the filling of the worked space may be an option to overcome the relevant difficulties in ensuring the stability of the side rocks and the preservation of haulage drifts. This approach is used in work [4], which considers the use of the filling of the worked space to increase the efficiency of coal seam treatment. However, by limiting themselves to the choice of means for mechanizing the filling operations, the researchers do not offer specific technical solutions aimed at ensuring the stability of preparatory workings.

Some experts believe that leaving the rock in a mine could solve the complex issues of geomechanical processes management in the coal-rock massif, which accommodates the workings in the development of treatment and preparatory operations [5]. It is noted that it is the filling of the worked space that provides the least shrinkage of the worked thickness and limits the displacement of side rocks in the array. However, this argument gives no solutions to ensure the stability of the side rocks and the operational condition of haulage drifts, especially with limited rock volumes in the mine.

To preserve the mining workings, under limited rock volumes, it is proposed to use a hardening filling in underground conditions [6]. This solution ensures the safety of workings due to the minimum shrinkage of the hardening support, designed to protect the drifts, in comparison with other types of filling. At the same time, there are still unresolved issues related to handling the filling hardening

process and preparing the multi-component hardening mixtures, as well as to the impact of hardening supports on the stability of haulage drifts.

As an alternative component of the filling, it is proposed to use the waste of the processing plants, which are placed in the worked space, formed after the excavation of the minerals [7]. The hydraulic technique of supplying such materials into the worked space ensures the satisfactory stability of filling arrays while the condition of workings somewhat improves. However, at the same time, as a result of the array formation, a water flow carries away small fractions of the material used to the haulage drifts, which requires the implementation of special measures to manage used water.

It is obvious that in order to ensure the stability of mining workings under difficult mining and geological conditions, it is necessary to focus on the use of pliable supports made from special materials, whose application would help reduce harmful manifestations of mountain pressure in haulage drifts. The results reported in work [8] indicate that the use of pliable supports of a certain rigidity, made from shredded filling material, to protect the workings creates zones of stable rocks in a coal-rock massif. However, they do not take into consideration the impact and change in the rigidity of protective structures on the formation of such zones of stability, especially when the dynamic loads manifest themselves when there are sudden displacements of the main roof.

All this suggests the relevance of research aimed at substantiating the stability of haulage drifts at different protection techniques, taking into consideration a change in the rigidity of protective structures, making it possible to limit the displacement of the stratified rocks over a preparatory working in the worked space.

---

## 3. The aim and objectives of the study

---

The aim of this study is to substantiate the conditions for the stability of a haulage drift of the steep coal seam with protective structures of different rigidity.

To accomplish the aim, the following tasks have been set:

- to investigate, using models made from equivalent materials, the stability of a coal seam roof with a pliable support under the action of dynamic loads;

- to examine, using models made from optical materials, the stressed-strained state of side rocks at the different techniques for protecting a haulage drift.

---

## 4. Materials and research methods to substantiate the stability conditions of haulage drifts

---

Under actual conditions of the development of steep coal seams, at the different techniques to manage mountain pressure in a breakage face, the safety of a haulage drift is ensured by the stability of the roof as the main load-carrying element of the underground structure. Haulage drifts are guarded by the coal pillars of limited size or wooden structures.

The set of technical solutions for the protection of section preparatory workings includes security facilities of different rigidity, designed to ensure the stability of haulage drifts under different conditions. In the absence of a possibility to leave the rock in a mine to improve the conditions of maintenance of haulage drifts, it is proposed to install, above

a preparatory working, above the pillars of coal or wood chocks made from sleepers, a supporting shell, which is filled with compressed air.

The elastic shell supporting the side rocks is a soft structure of the predefined size and shape, whose walls are limited by two surfaces (the roof and soil of the worked layer), the distance between which is small compared to other dimensions. Such a soft structure, if filled, for example, with compressed air, can perceive stretching stresses under working pressure and resist the force compressing loads [9].

Under actual conditions of developing steep coal seams, an important operational characteristic of such a shell is the number of degrees of freedom that take into consideration the displacements of the system in space, which depends on fixing techniques. It can be considered that the shell under consideration is fixed by generatrix, when its fixation is provided, while the elastic compressed medium, enclosed in such a structure, renders it rigidity, that is, the ability to resist external exerting force loads.

There are three states of the elastic shell. The initial state is when the pressure in the shell is close to the atmospheric and compensates for its own mass. The original state is when, for example, the pressure of compressed air in the shell reaches the operational level. The final state is if the balance is ensured under the influence of applied external loads.

Earlier studies have found [9, 10] that as a result of external influence on the supported structure, its stability is ensured by the presence of a pliable base. However, if a shell airtight container filled with compressed air is used as a pliable base, any displacement of the supporting structure creates a pressure gain in the shell, proportional to its displacement. In cases where compressed air in a container is completely isolated, no absorption of energy can occur. If there are small leaks of compressed air, the pressure increment would correspond to the losses resulting from these leaks, and the compressed air capacity would act as a damper [11].

Given this, it can be assumed that the use of elastic supporting shells filled with compressed air would ensure the stability of side rocks and section preparatory workings (including haulage drifts) in the development of steep coal seams.

To assess protective structures as a means for limiting the displacement and deformation of side rocks and their effect on the stability of haulage drifts, a set of laboratory experiments has been performed, using models made from equivalent and optical materials.

Studies on models made from equivalent materials were performed to assess the impact of a support on the stability of side rocks under the action of dynamic loads. The selection of material for the models is carried out in accordance with the recommendations given in [12, 13]. According to the hypothesis of the beams [14], it can be assumed that in a breakage face the roof of a coal seam is deformed and destroyed similarly to beams, with all sorts of variants of support bonds.

Based on this position, the roof rocks were represented in the form of a beam, of length  $L_b=0.6$  m, thickness  $h=0.02$  m, width  $b=0.04$  m. The mass of the beam corresponded to  $m_b=1.4$  kg, the elasticity module is  $E=8,800$  MPa, density is  $\rho=2,100$  kg/m<sup>3</sup>. The beam was made from a sand-cement mixture; the models used in the experiments met the criteria of similarity [15].

The stability of the roof rocks was studied on models in which the beam at one end had a hard pinch, the other end

rested on a support made from crushed rock with different particle size distribution. As an alternative, we considered the models in which the free end of the beam rested on a wooden structure and an elastic supporting shell, directed by compressed air. The photograph of the bench to study the stability of the roof with a pliable support is given in Fig. 1.

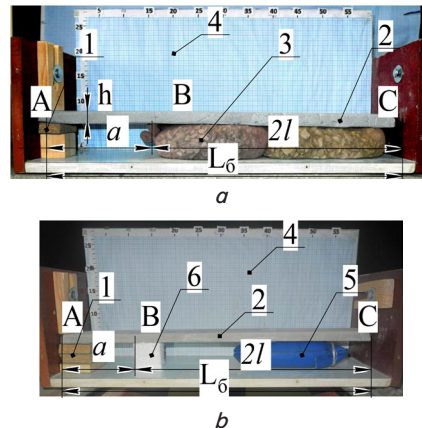


Fig. 1. Photograph of the bench to study the stability of the roof of a coal seam: *a* – with a support made from crushed rock; *b* – with a supporting shell filled with compressed air: 1 – rigid fastening of the beam; 2 – beam – direct roof; 3 – a support made from crushed rock; 4 – coordinate grid; 5 – an elastic supporting shell filled with compressed air; 6 – wood chock;  $L_b$  – length of the beam,  $L_b=0.6$  m;  $h$  – thickness of the beam,  $h=0.02$  m;  $a$  – the beam span is  $a=0.2$  m

The granulometric composition of the filling material made from crushed rock for a support that holds the beam, its bulk density  $\rho_{b.d.}$  (kg/m<sup>3</sup>) and voidness  $M$  (%), were determined in accordance with [16]. The compaction ratio  $k_{comp}$  of the filling material was calculated as the ratio of the volume, occupied by the rock mass before compaction, to the volume that it occupied after the compaction.

To determine the compaction ratio, we used the starting material when the crushed rock consisted of heterogeneous fractions and the material sieved into standard fractions. Special steel cylinders were used for testing, in which crushed rock was poured; we placed them between the slabs on the press and compressed them.

Models made from optically sensitive material were used to determine the stressed-strained state of the side rocks, in a coal-rock massif that can accommodate workings. Igdantin (composition: glycerin, gelatin, and water) was used as such a material. The models were examined at the polarizing installation PPU-4, by a known way of comparing colors and the bands of tangent stress distribution. The criteria of similarity, the elastic and optical constants of the models were determined in accordance with the methodology developed at the Skochinsky Institute of Mining [11].

The models, taken in the form of parallelepipeds, measuring 300×300 mm and 20 mm thick, were loaded according to the scheme when the vertical load corresponded to the depth  $H=1200$  m and the horizontal load was created by the rebuff of the side walls of the model. The distribution of stresses was studied in the vicinity of a haulage drift, passed on the coal seam with a capacity of  $m=1.0$  m. The arch-shaped drift: height, 2.5 m; width, 2.5 m. The study was carried out on models with layers that were taken as im-

itators of the direct and main roof and soil of the coal seam, with a capacity of  $2m$  and  $4m$ . The models simulated a haulage drift protected by pillars of coal or a filling array made from crushed rock. The height of the pillar of coal was  $h=6m$ , where  $m$  is the power of a coal seam,  $m$ ; the rigidity in the model is  $c=150$  N/m. The filling array made from crushed rock, whose rigidity corresponded to  $c=50$  N/m, was arranged over the entire floor height above a haulage drift.

The conditions of haulage drift stability were also determined on models when the working was protected by pillars of coal or wood chocks made of sleepers. The rigidity of the wooden structures corresponded to  $c=50$  N/m; they were laid out over the working in two rows. Above the pillars of coal or bonfires, we placed an elastic supporting shell, designed to limit the displacement of side rocks in the lower and middle part of the long face for the height of the floor. When modeling the stability of haulage drifts, the final state of the simulated limited-rigidity shell (N/m) was taken into consideration. To this end, we used an elastic cylindrical hollow tube with different thickness walls, whose diameter corresponded to the simulated power of the layer. The scale of the simulation corresponded to M1:100.

Options for protection a haulage drift are given in Table 1.

Table 1

Modeled options for protecting a haulage drift

Protection technique	Rigidity $c_1$ , N/m	The rigidity of supporting shell $c_2$ , N/m
Pillars of coal – supporting shell	150 pillars of coal	25
		50
		75
		100
Wood chocks made from sleepers – supporting shell	50 wood chocks made from sleepers	25
		50
		75
		100

In the analysis of a static field of the tangent strains in a coal-rock massif containing workings, it was taken into consideration that the volumetric stressed state of the side rocks changes, in proportion to the distance from a working contour, from a state close to the generalized stretching to the generalized compression in the depth of the array [17, 18].

A comprehensive approach was used to assess the stressed-strained state of the side rocks and the stability of haulage drifts, where known methods of processing experimental data were applied to process the results of physical modeling and analytical calculations were carried out using the fundamental provisions from mining geomechanics, the theory of elasticity and vibrations.

## 5. Results of studying the stability conditions for haulage drifts

### 5.1. Results of studying the stability of the roof with a pliable support

Fig. 1 shows that the beam at point A has a rigid fastening, and its loose end C rests on a filling array of crushed rock (Fig. 1, a) or a wooden protective structure and an elastic supporting shell filled with compressed air (Fig. 1, b). The beam span AB is equal to  $a=0.2$  m (Fig. 1).

Laboratory data to determine the granulometric composition of the crushed rock, its bulk density, ( $\text{kg/m}^3$ ), and voidness  $M$ , are given in Tables 2, 3. For each fraction size, 10 tests were performed. The number of tests  $n=10$ , required to obtain sufficient modeling results, with an accuracy score of 5 %, was established in accordance with [19].

The compaction coefficient of crushed rock was established during its compression [20], when with an increase in bulk density  $\rho_{b.d.}$  ( $\text{kg/m}^3$ ) and voidness  $M$  (%) of the filling material, the compaction coefficient increased from  $k_{comp}=1.49$  to the maximum values  $k_{comp}=1.53$ , at the heterogeneous fractions of crushed rock. The values of the compaction coefficient decrease to  $k_{comp}=1.13$  with an increase in  $\rho_{b.d.}$ , ( $\text{kg/m}^3$ ), and a decrease in  $M$  (%), which is typical for homogeneous fractions of small sizes (0.1–1 mm).

Table 2

The granulometric composition of the crushed rock

Fraction size, mm	>5	5–4	4–3	3–2	2–1	1–0.1
Percentage, %	1	17	22	25	23	12

Table 3

Laboratory test data on crushed rock

Number of entry	Fraction size, mm	Bulk density $\rho_{b.d.}$ , $\text{kg/m}^3$	Voidness $M$ , %
1	5–4	1,680	20
2	4–3	1,740	18
3	3–2	1,870	11
4	2–1	1,880	11
5	1–0.1	1,990	6
6	5–0.1	1,840	13

In the laboratory, a load of  $m=2.4$  kg was used to determine the static stiffness  $C_{os}$  (N/m) of the elastic shell filled with compressed air. The load was applied to the simulated structure, and the method of photo-registration [21] was applied to determine the magnitude  $X$  (m), that is, the amount of shell compression under loading. Before the tests, the shell was filled with compressed air. Using a gauge, the pressure in the shell was measured. For each working pressure in the shell, 10 measurements were performed to determine the magnitude  $C_{sh}$  (N/m). Laboratory data are given in Table 4. The variation rate was 5 %.

Table 4

Laboratory test data to determine the static stiffness of a supporting shell

No. of entry	Working pressure in a shell, kPa	Load mass $m$ , kg	Magnitude $X$ , m	Static stiffness of the shell $C_{sh}^{st}$ , (N/m)
1	50	2.4	0.0018	13,000
2	30	2.4	0.0034	7,000
3	20	2.4	0.0052	4,500
4	10	2.4	0.0065	3,600

The rigidity of the wooden structure was determined in a similar way and amounted to  $C_W=7,000$  N/m.

To determine the dynamic rigidity of the simulated system, we established the magnitude of beam displacement  $X$ , (m), when a rock block of different mass  $m$ , (kg),



was dropped on it from the height  $H=0.3$  m we registered an inelastic impact.

When testing models, the displacements of the beam  $X$ , (m), were recorded by a digital camera. Based on the photographic images, using pixel coordinates of the dots, applying the basic principles of photogrammetry [21], we determined the beam position in space before and after the action of the external force on it. Experimental data are given in Tables 5, 6.

Table 5

Laboratory data to determine the displacement magnitude of beam  $X$ , (m), with a support made from crushed rock, when dropping a load of weight  $m=0.46$  kg

Indicator	Fraction size, mm					
	5-4	4-3	3-2	2-1	1-0.1	5-0.1
Displacement $X$ , (m)	0.003	0.0032	0.0028	0.002	0.0016	0.0038
Dynamic stiffness $C$ , (N/m)	6,000	5,600	6,500	9,100	11,400	4,800

Table 6

Laboratory data to determine the displacement magnitude of beam  $X$ , (m), with a support in the form of a shell filled with compressed air

No. of entry	Mass of a falling load $m$ , kg	10 kPa	20 kPa	30 kPa	50 kPa
		$X$ , m	$X$ , m	$X$ , m	$X$ , m
1	0.1	0.0009	0.00062	0.00042	0.0003
2	0.13	0.0012	0.00081	0.00048	0.00042
3	0.17	0.0016	0.0011	0.00051	0.00046
4	0.2	0.0021	0.0016	0.00062	0.00052
5	0.46	0.0026	0.0021	0.0007	0.0009
6	0.7	0.0038	0.0024	0.0009	0.0011

The beam displacement  $X$ , (m), recorded in the experiments, corresponds to the equivalent static force  $P_{eq}$ , (N), the magnitude of which can be determined from the following expression, similarly to [22-24].

$$P_{eq} = S \cdot p, \tag{1}$$

where  $S=m \cdot V$  is the magnitude of the impact pulse, kgm/s;

$$p = \sqrt{\frac{g}{x}},$$

$p$  is the frequency of the beam's natural oscillations in the examined system, 1/s.

Data from experimental studies are given in Tables 7, 8.

After the force influence of a falling load on the beam, the duration of the impact can be determined, as in [8], from the following expression

$$t_{imp} = \frac{\pi}{2} \sqrt{\frac{x}{g}}, \tag{2}$$

and the magnitude of the maximum compression of a pliable support due to the impact – from the following expression [23]

$$\Delta X = \frac{m_b g}{c} + \sqrt{\frac{m_b^2 g^2}{c^2} + 2gH} \frac{m^2}{c(m+m_b)}. \tag{3}$$

The physical process of the beam's natural vibrations in the examined system, when an elastic supporting shell with compressed air is used, is characterized by its goodness  $G$ , the value of which is determined from the following expression [22, 24].

$$G = \frac{2\pi}{\delta}, \tag{4}$$

where  $\delta$  is the logarithmic decrement of fading.

The magnitude of force  $P_{imp}$ , (N), from the impact of a load weighing  $m$ , (kg), against the beam when falling from a height of  $H=0.3$  m, can be determined using Newton's second law [23], when

$$m dV = P dt. \tag{5}$$

Using a theorem of the average [22, 23], we believe that the force of the impact is determined as

$$P_{imp} = \frac{1}{2} \cdot \frac{mV}{t_{imp}}, \tag{6}$$

where  $t_{imp}$  is the impact duration, s.

Table 7

Values of the equivalent static force  $P_{eq}$  (N) to compress a support made from crushed rock

Mass of a falling load $m$ , kg	Fraction size, mm	Beam displacement $X$ , m	The magnitude of the equivalent static force $P_{eq}$ , (N)
0.46	5-4	0.003	63.7
	4-3	0.0032	61.7
	3-2	0.0028	66
	2-1	0.002	78
	1-0.1	0.0016	87.2
	5-0.1	0.0038	56.6

Table 8

Values of the equivalent static force  $P_{eq}$  (N) for compressing a supporting shell, filled with compressed air, under different working pressure

Mass of a falling load $m$ , kg	Equivalent static force $P_{eq}$ (N)							
	Working pressure in a supporting shell, kPa							
	10 kPa		20 kPa		30 kPa		50 kPa	
	$X$ , (m)	$P_{eq}$ , (N)	$X$ , (m)	$P_{eq}$ , (N)	$X$ , (m)	$P_{eq}$ , (N)	$X$ , (m)	$P_{eq}$ , (N)
0.1	0.0009	25.3	0.00062	30.4	0.00042	37	0.0003	48.1
0.13	0.0012	28.4	0.00081	34.6	0.00048	45	0.00042	48.8
0.17	0.0016	32.2	0.0011	38.9	0.00051	57.2	0.00046	60.2
0.2	0.0021	33.1	0.0016	37.9	0.00062	61	0.00052	66.5
0.46	0.0026	68.4	0.0021	76.2	0.0009	116.3	0.0007	131.2
0.7	0.0038	86.2	0.0024	108.4	0.00098	178.2	0.0011	160.2

Fig. 2 shows the dependences that reflect a change in the maximum compression of a pliable support  $\Delta X$  (m) and the impact duration  $\Delta t_{imp}$  (s) on its dynamic stiffness  $C$  (N/m).

It was determined experimentally that with an increase in the dynamic rigidity of a pliable support  $c$  (N/m) the

magnitude of its maximum compression  $\Delta X$  (m) and the period  $\Delta t_{imp}$  (s), during which the compression occurs, decrease (Fig. 2, a-c).

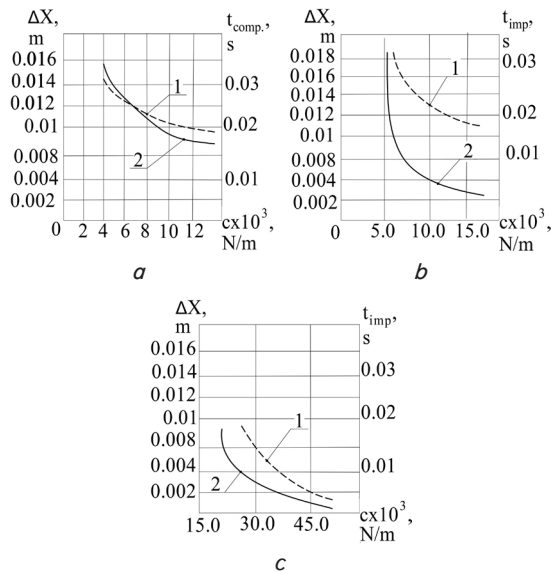


Fig. 2. Plots of change in the maximum compression of a pliable support  $\Delta X$  (m) and the impact duration  $\Delta t_{imp}$  (s) when dropping a load of weight  $m$ , (kg), from height  $H$ , (m), on its dynamic rigidity  $c$  (N/m): a – crushed rock; b – elastic shell, filled with compressed air, with a working pressure of 10 kPa; c – elastic shell, filled with compressed air, with a working pressure of 50 kPa; 1 –  $\Delta t_{imp}$  (s); 2 –  $X$  (m)

Fig. 3 shows the plots of change in the values of goodness  $G$  of the examined system dependent on its dynamic rigidity, while the beam is maintained by an elastic shell.

It was established that at the minimal dynamic rigidity  $c=5.0$  N/m the goodness of the system is equal to  $G=380$  (Fig. 3). With the increase in dynamic rigidity, the goodness  $G$  of the system increases and, at  $c=45,000$  N/m, reaches the maximum values when  $G=1,000$  (Fig. 3, b). At these  $G$  values, the probability of the system destruction increases.

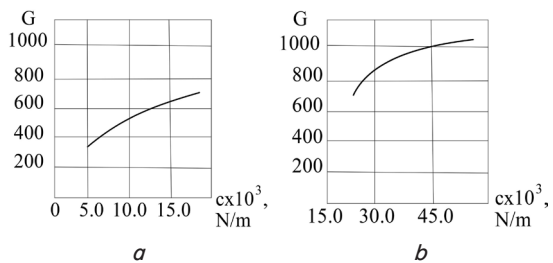


Fig. 3. Plots of changes in the magnitude of goodness  $G$  of the examined system with an elastic shell dependent on its dynamic rigidity  $c$  (N/m): a – at a working pressure in the shell of 10 kPa; b – at a working pressure in the shell of 50 kPa

Fig. 4 shows the plots reflecting a change in the equivalent static force  $P_{eq}$  (N) depending on the rigidity of a support  $c$  (N/m), which demonstrate that the increasing rigidity increases the equivalent force. It was registered that for a beam with a support made from crushed rock, when the rigidity of such a support increases from  $c=4,800$  N/m to  $c=12,000$  N/m, the magnitude of the

equivalent static force  $P_{eq}$  (N) changes from  $P_{eq}=58$  N to  $P_{eq}=84$  N (Fig. 4).

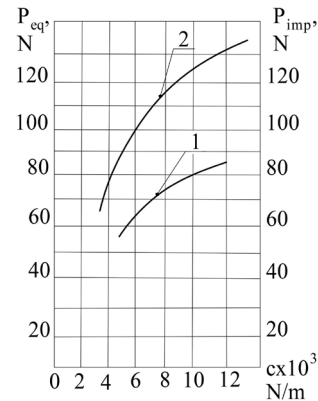


Fig. 4. Plots of changes in the equivalent static force  $P_{eq}$  (N) depending on the rigidity of a support  $c$  (N/m): 1 – made from crushed rock; 2 – elastic supporting shell

When using an elastic shell filled with compressed air, at this interval of rigidity variations, the equivalent static force changes from  $P_{eq}=82$  N to  $P_{eq}=131$  N (Fig. 4).

In all cases, the dynamics coefficient values range from  $k_{din}'1.5$  to  $k_{din}'2.7$ , with a lower rigidity of the supporting support ratio being less than the dynamic factor.

**5. 2. Results of studying the stressed-strained state of side rocks**

The results of studying the stressed-strained state of side rocks at the different protecting techniques of haulage drifts are given in the form of a static field of tangent strains, which were recorded in the models of a coal-rock massif that can accommodate workings.

Fig. 5, a, b shows the diagrams of models of the static field of tangent strains in the vicinity of a haulage drift when protecting with pillars of coal (Fig. 5, a) or by filling the worked space (Fig. 5, b).

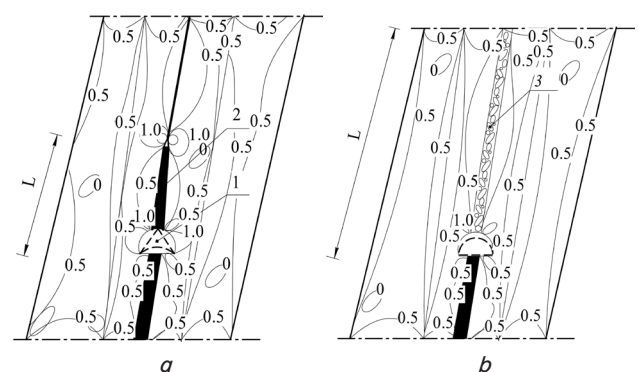


Fig. 5. Schematic of the static field of tangent strains in a coal-rock massif when protecting a haulage drift: a – by pillars of coal; b – by filling the worked space; 1 – haulage drift; 2 – pillar of coal; 3 – filling array; the stiffness of a pillar of coal is  $c_p=150$  N/m; the rigidity of a filling array is  $c_a=50$  N/m; the height of a pillar of coal in the model is  $h=0.03$  m;  $L$  – length of the roof section maintained by a protective structure, m

The study of the diagrams of the models of stress distribution in the vicinity of a haulage drift when protecting by

pillars of coal shows that the greatest tangential stresses are concentrated near the contour of a working and at the edge of a pillar of coal, in the place of bending the rocks of the roof and the soil of the coal seam (Fig. 5, a). Using the filling of the worked space to maintain the side rocks reduces the concentration of stresses in the rocks of the roof and soil along the entire length of the breakage face, as well as in the vicinity of a haulage drift (Fig. 5, b).

Fig. 6 shows a model of the static field of tangent strains in a coal-rock massif when protecting a drift by a pillar of coal and a supporting elastic shell.

Analysis of the static stress field at this combination of protective elements indicates that the concentrations of stresses in the roof and soil match the bottom of the drift, where the side rocks are supported by a pillar of coal. Above the pillar of coal, in the area where the supporting shell is located, we have a smooth deflection of the side rocks and a zone with a minimum concentration of stresses in the rocks of the roof and soil (Fig. 6).

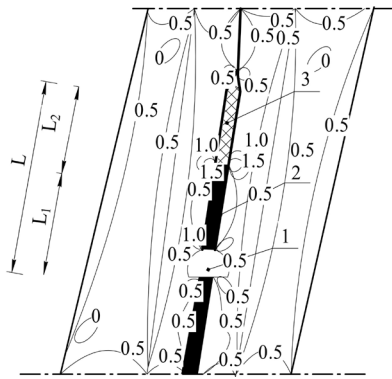


Fig. 6. Schematic of a model of the static field of tangent strains in a coal-rock massif when a haulage drift is protected by the pillars of coal and a supporting shell, when the stiffness of the shell is equal to  $c_{ss}=50 \text{ N/m}$ ;  $L=L_1+L_2$ , where  $L_1$  is the height of a pillar of coal, m;  $L_2$  is the shell length, m; 1 – haulage drift; 2 – pillar of coal; 3 – elastic supporting shell

When protecting a section preparatory working by the wood chocks made of sleepers, in combination with a supporting shell (Fig. 7, a–c), the concentration of stresses in the side rocks is markedly reduced, in comparison with the protection of the drift by the pillars of coal and a shell. This occurs as a result of a smooth bend of the side rocks throughout the entire area of roof maintenance, the length of which  $L$ , (m). This effect is achieved by increasing the area of contact between the roof and the soil with a pliable protective structure located above the haulage drift.

However, the most favorable conditions for maintaining the workings are created at a certain rigidity of the supporting shell, when its magnitude is equal to the rigidity of the wood chocks or less (Fig. 7, a, b).

When a haulage drift is protected by wood chocks and a supporting shell, whose rigidity is 1.5 times larger than the rigidity of wood chocks, the maximum concentration of stresses moves to the area of the shell installation. At the

bottom of the drift, where the wood chocks made from sleepers are placed, we have a minimum concentration of stresses due to their compression (Fig. 7, c).

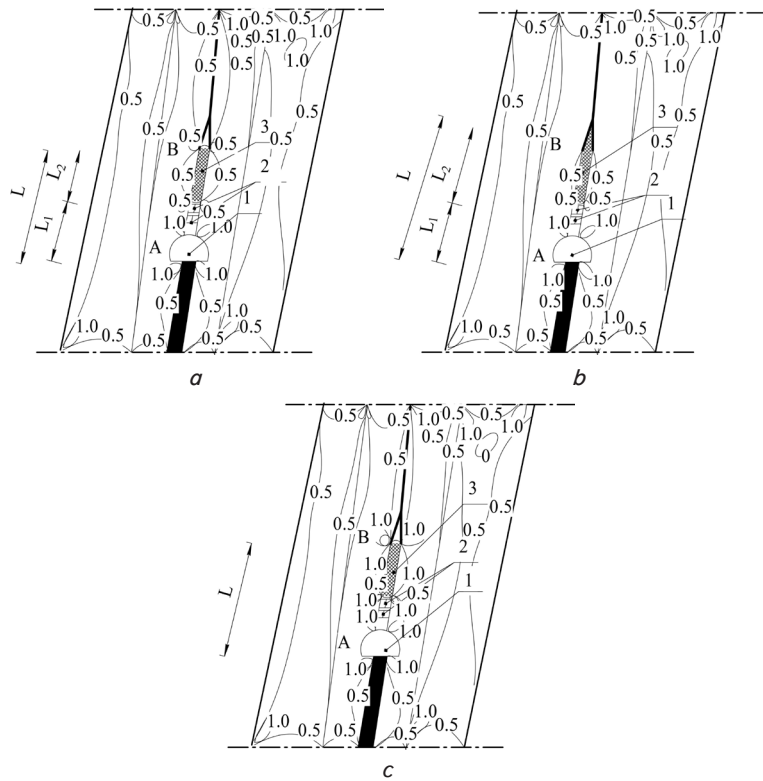


Fig. 7. Schematic of a model of the static field of tangent strains in a coal-rock massif when protecting the haulage drift by wood chocks made from sleepers (the rigidity of wood chocks made from sleepers is  $c_{ps}=50 \text{ N/m}$ ) and a supporting shell, when *a* is the rigidity of a shell  $c_s=50 \text{ N/m}$ ; *b* is the stiffness of a shell  $c_s=25 \text{ N/m}$ ; *c* is the stiffness of a shell  $c_s=75 \text{ N/m}$ ; 1 – haulage drift; 2 – wood chocks made from sleepers; 3 – elastic supporting shell;  $L$  is the length of the supported section of the roof, m;  $L_1$  – by wood chocks, m;  $L_2$  – by a supporting shell, m

It is believed [25] that the stressed-strained state of the side rocks in a coal-rock massif, which can accommodate workings, depends on the rigidity of protective structures and the magnitude of deflection of the rock layers. The degree of impact of the rigidity of protective structures on the distribution of stresses in the model, when the bending rigidity of the roof and soil does not change, is proposed to be assessed, similarly to [25], by a factor  $k_M^i$ , using the following expression

$$k_M^i = \frac{cL^3}{EI}, \tag{7}$$

where  $c$  the stiffness of a pillar of coal or a filling massif, N/m;  $EI$  is the bending rigidity of the roof rocks,  $\text{N}\cdot\text{m}^2$ ;  $L$  is the length of the roof section maintained by a pillar of coal or a filling array of the roof section, m.

Fig. 8, a, b shows the plots reflecting a change in the ratio  $k_M^i$  in the model depending on the parameter  $L$ , (m).

The dependences, given in Fig. 8, a, reflect a change in the coefficient  $k_M^i$  depending on the parameter  $L$ , (m), determined from expression (7), when the values of  $L$  (m) in the model changed from  $L=0.02 \text{ m}$  to  $L=0.18 \text{ m}$  at the

following rigidity of protective structures: pillars of coal,  $c=150$  N/m, a filling massif,  $c=50$  N/m. When a haulage drift is protected by pillars of coal, with an increase in the  $L$  (m) parameter in the model from  $L=0.02$  m to  $L=0.18$  m, the  $k_M^\tau$  coefficient values change from  $k_M^\tau=0.00001$  to  $k_M^\tau=0.0038$ , that is, they increase (Fig. 8, *a*, dependence 1). When adopting the filling of the worked space to protect a haulage drift, the array undergoes a geomechanical change, leading to a decrease in the values of the coefficient  $k_M^\tau$  from  $k_M^\tau=0.00002$  at  $L=0.02$  m to  $k_M^\tau=0.0013$  at  $L=0.18$  m (Fig. 8, *a*, dependence 2).

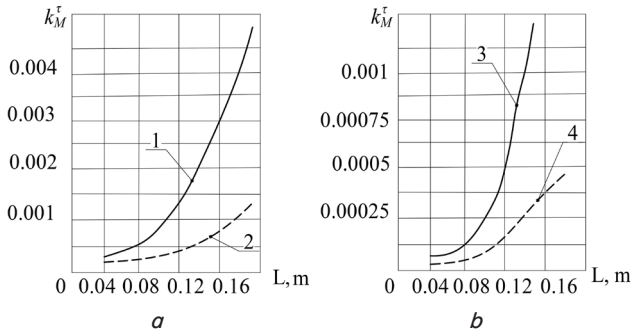


Fig. 8. Plots of change in the coefficient  $k_M^\tau$  in the model depending on the parameter  $L$ , (m): *a* – haulage drift is protected by pillars of coal or a filling array made from crushed rock; *b* – a haulage drift is protected by pillars of coal and a supporting shell or by wood chocks and a supporting shell; 1 – the rigidity of a pillar of coal is  $c=150$  N/m, 2 – a filling array made from crushed rock with the rigidity of  $c=50$  N/m; 3 – the rigidity of a pillar of coal is  $c_1=150$  N/m, the stiffness of a shell is  $c_2=75$  N/m; 4 – the rigidity of wood chocks is  $c_1=50$  NM, the stiffness of a shell is  $c_2=25$  N/m

The use of pillars of coal or wood chocks made from sleepers, combined with a supporting shell, gives completely different values of the coefficient  $k_M^\tau$ , to be determined from the following expression

$$k_M^\tau = \frac{c_1 L_1^3 + c_2 L_2^3}{EI}, \tag{8}$$

where  $c_1$  is the rigidity of a pillar of coal or wood chocks, N/m;  $c_2$  is the stiffness of an elastic shell, N/m;  $L_1$  is the length of a section of the roof maintained by a pillar of coal or a wooden structure, m;  $L_2$  is the length of a section of the roof maintained by an elastic shell, m.

The models helped establish that an increase in the size of the shell, located above a pillar of coal or wood chocks, from  $L_2=0.04$  m to  $L_2=0.18$  m, leads to an increase in the stiffness factor  $k_M^\tau$ . When a haulage drift is protected by pillars of coal (the rigidity of a pillar of coal is  $c_1^p = 150$  N/m) in combination with a shell, the value of the factor studied vary from  $k_M^\tau=0.00008$  to  $k_M^\tau=0.0015$  (Fig. 8, *b*, dependence 3).

When using wood chocks, the rigidity of which is equal to  $c_1^{ns} = 50$  N/m, in combination with a supporting shell of rigidity  $c_2^s = 25$  N/m, the  $k_M^\tau$  coefficient values vary from  $k_M^\tau=0.00006$  to  $k_M^\tau=0.00048$  (Fig. 8, *b*, dependence 4). It is obvious that with the increase in the size of the pliable protective structures supporting the roof of the coal seam, the values of the coefficient  $k_M^\tau$  take the minimum values, but only when one registers an increase in the size of the

area of the bend of the side rocks. At small  $L$  (m) parameters, when  $L=0.02-0.04$  m, the  $k_M^\tau$  coefficient values are almost the same for all simulated protective options (Fig. 8, *a*, *b*).

Fig. 9 shows the plots that reflect a change in the coefficient  $k_M^\tau$  in the model depending on the rigidity variation in a supporting shell. The dependences, shown in Fig. 9, are derived from expression (8) when  $L=L_1+L_2$  and  $L_1=L_2$ . The parameter  $c_1$ , (N/m), corresponded to a specific protection technique of a haulage drift while the parameter  $c_2$ , (N/m), changes.

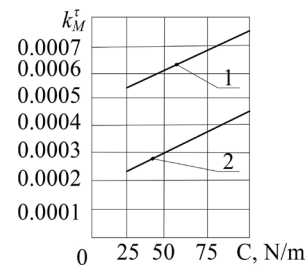


Fig. 9. Plots of change in the coefficient  $k_M^\tau$  in the model depending on the variation of the rigidity of the protective structures erected above a drift: 1 – when protecting by pillars of coal and a supporting shell; 2 – when protecting by wood chocks made from sleepers and a supporting shell

Our experiments suggest that at the rigidity of a pillar of coal  $c_1=150$  N/m and the stiffness of a shell  $c_2=75$  N/m, the coefficient  $k_M^\tau=0.0007$ . When the wood chocks made from sleepers are used to protect a haulage drift, at their rigidity  $c_1=50$  N/m and the stiffness of an elastic shell  $c_2=25$  N/m, the value of the examined coefficient  $k_M^\tau=0.00022$  (Fig. 9). As one can see, an increase in the rigidity of protective structures leads to an increase in the coefficient  $k_M^\tau$ , which means that the variation of their parameters changes the nature of the distribution of stresses in a coal-rock massif, which can accommodate workings.

## 6. Discussion of results of studying the justification of the stability conditions of haulage drifts

The result of our laboratory studies involving models made from equivalent and optical materials is the performed physical simulation of geomechanical processes that cannot be investigated in mine conditions (Fig. 1, 5–7).

It was registered that the stability of the simulated geomechanical system, in which the roof of a coal seam is represented in the form of a beam (Fig. 1), which has pliable support links, depends on the rigidity of the support. At an inelastic impact, with increasing rigidity of the pliable support, the displacements of the roof decrease (Fig. 2). Meanwhile, under such conditions, with the dynamic impact on the roof, there is an increased likelihood of destruction of side rocks and their chaotic displacement to the working (Fig. 4).

Maximum roof displacements depend on the amount of supports' pliability (Tables 5, 6). When the filling arrays are used to maintain side rocks, the amount of their pliability is determined by a compaction factor, taking into consideration the granulometric composition of the crushed rock (Table 5). In the case when elastic shells filled with compressed air are used to maintain the side rocks, the mallea-



bility of such structures depends on the amount of working pressure in them (Table 6).

The presence of pliable supports over a haulage drift (Fig. 7) or the use of the filling of the worked space (Fig. 5, *b*) contributes to the preservation of the stability of side rocks and the operational state of mining workings. However, the larger the carrying capacity of protective structures and their rigidity, the greater the destructive efforts that the side rocks are exposed to in the zones of excessive stresses (Fig. 5, *a*, Fig. 6). Such zones are formed through a contact between the rigid means of protection and side rocks over a haulage drift, as a result of minimal deflection of the roof rocks of a coal seam.

The preservation of haulage drifts in the operational state is ensured by the presence of protective structures of certain sizes and rigidity in the worked space (7), Fig. 8. With an increase in the area of bend of the side rocks over a haulage drift and while limiting their displacements, there is a decrease in the concentration of stresses in the array, that is, the stressed-strained state of the side rocks changes (Fig. 5, *b*, Fig. 7, *a*, *b*).

A change in the stressed-strained state of side rocks when applying pliable supports occurs as a result of their shrinkage or compression. In order to achieve a favorable geomechanical condition in a coal-rock massif containing the workings, it is necessary to ensure a smooth deflection of the roof rocks throughout the height of the floor (Fig. 5, *b*).

Therefore, all other things being equal, the probability of manifestations of natural hazards in workings will always be greater in the absence of pliable supports in the worked space. The absence of the latter leads to a deterioration in the stability of the roof and haulage drift, which increases the likelihood of a working's blockage.

Thus, the presence of pliable protective structures over a haulage drift, as opposed to conventional protection techniques (for example, pillars of coal), ensures the stability of side rocks, prevents their stratification, and blockages of mining workings.

The use of the filling, made from the crushed rock, of the worked space, in comparison with the hardening filling, contributes to the reduction of harmful manifestations of mountain pressure in a coal-rock massif, especially at the sudden collapses of thickness, when there are dynamic loads. When the filling arrays are used to maintain the side rocks, whose compaction coefficient  $k_{comp}=1.5-1.53$ , a smooth bend of the roof over the drift is ensured (Fig. 5, *a*).

With the limited rock volumes in a mine, which is used to fill the worked space, the application of a supporting elastic shell above the drift provides stability of the workings (Fig. 7). Performing the role of a dampener, the supporting shell allows for a smooth bending of the side rocks over the drift, as is the case when filling the worked space. At the same time, the destruction of the roof and its collapse into the working is practically excluded. This effect cannot be achieved by using pillars of coal or a hardening filling to protect the section preparatory workings.

Meanwhile, the efficiency of the use of such shells, once installed in the worked space, would increase if their rigidity is adjusted. However, such a solution requires further research.

The recommended protection techniques of section preparatory workings (Fig. 7) are low-cost and make it possible to ensure the operational condition of haulage drifts in the development of steep coal seams (the inclination angle of such seams is  $\alpha=55-70^\circ$ ).

---

## 7. Conclusions

---

1. Our study, which involved models made from equivalent materials, into the stability of the roof of a coal seam with a pliable support under the action of dynamic loads has established that increasing the rigidity of the support increases its carrying capacity. The maximum impact force values ( $P_{imp}=80-120$  N) and the greatest goodness of the simulated system ( $G=600-1,000$ ) have been observed at the minimal displacements of the roof. This has a negative impact on the resilience of the side rocks in a coal-rock massif containing the workings, especially at the sudden collapses of the stratified thickness.

2. The application of the filling of the worked space or the wood chocks made from sleepers, located above the drift, in combination with an elastic supporting shell, filled with compressed air, provides a reduction in the concentration of stresses in a coal-rock massif. This result is achieved by increasing the area of the bend of the roof and soil of a coal seam and by increasing the area of their contact with the pliable means of protection. Variation of the rigidity of the elastic supporting shell significantly changes the nature of the distribution of stresses in a coal-rock massif, even at the same dimensions of protective structures (for example, pillars of coal), due to the bend of the roof of the coal seam.

---

## References

1. Zinchenko, Yu. I., Sudin, M. S., Zinchenko, A. Yu. (2011). Perspektiva razvitiya shaht Tsentral'nogo rayona Donbassa. Ugol' Ukrainy, 12, 35–38.
2. Liashok, Y., Iordanov, I., Chepiga, D., Podkopaiev, S. (2018). Experimental studies of the seam openings competence in different methods of protection under pitch and steep coal seams development. Mining of Mineral Deposits, 12 (4), 9–19. doi: <https://doi.org/10.15407/mining12.04.009>
3. Sotskov, V., Gusev, O. (2014). Features of using numerical experiment to analyze the stability of development workings. Progressive Technologies of Coal, Coalbed Methane, and Ores Mining, 401–404. doi: <https://doi.org/10.1201/b17547-68>
4. Dzyuba, S. V., Shmelev, N. A., Koval', N. V. (2012). Analysis of technology of underground development of mineral deposits for mining work in difficult geological conditions. Geotekhnicheskaya mehanika, 101, 284–291.
5. Zhukov, V. E. (2001). Ob odnoy strategicheskoy oshibke v razreshenii problemy razrabotki krutyyh plastov. Ugol' Ukrainy, 7, 6–10.
6. Krupnik, L. A., Shaposhnik, Y. N., Shaposhnik, S. N., Tursunbaeva, A. K. (2013). Backfilling technology in Kazakhstan mines. Journal of Mining Science, 49 (1), 82–89. doi: <https://doi.org/10.1134/s1062739149010103>

7. Blyuss, B., Semenenko, Eu., Nykyforova, N. (2008). The calculation procedure of hydrotransport parameters of bulk solids using hydrodynamically active additives solutions. Papers presented at the 14th International Conference on Transport and Sedimentation of Solid Particles. Saint Petersburg, 41–48.
8. Podkopaiev, S., Gogo, V., Yefremov, I., Kipko, O., Iordanov, I., Simonova, Y. (2019). Phenomena of stability of the coal seam roof with a yielding support. *Mining of Mineral Deposits*, 13 (4), 28–41. doi: <https://doi.org/10.33271/mining13.04.028>
9. Shpakov, V. P.; Fedyukin, D. L. (Ed.) (1986). *Klassifikatsiya pnevmaticheskikh konstruksiy. Primenenie RTI v narodnom hozyaystve*. Moscow: Himiya, 240.
10. Henderson, Dzh., Nashif, A., Dzhouns, D. (1988). *Dempfirovaniye kolebaniy*. Moscow: Mir, 448.
11. Haimova-Mal'kova, R. I. (1970). *Metodika issledovaniy napryazheniy polyarizatsionno-opticheskim metodom*. Moscow: Nauka, 116.
12. Glushihin, F. P., Kuznetsov, G. N., Shklyarskiy, M. F. et. al. (1991). *Modelirovaniye v geomehanike*. Moscow: Nedra, 240.
13. Basov, V. V., Rib, S. V. (2016). Selection of equivalent material for physical modeling of geomechanical processes in the vicinity of the mine workings of coal mines. *Bulletin of the Siberian State Industrial University*, 4, 32–35.
14. Shashenko, A. N., Pustovoytenko, V. P., Sdvizhkova, E. A. (2016). *Geomehanika*. Kyiv: Noviy druk, 528.
15. Borschch-Komponiets, V. I. (2013). *Prakticheskaya mehanika gornyh porod*. Moscow: Gornaya kniga, 322.
16. Hrebonkin, S. S., Havrysh, M. M. (Eds.) (2004). *Mekhanika hirsykykh porid. Vol. 1*. Donetsk: DonNTU, 169.
17. Baklashov, I. V. (1988). *Deformirovaniye i razrusheniye porodnykh massivov*. Moscow: Nedra, 271.
18. Kleppner, D., Kolenkow, R. J. (2012). *An Introduction to Mechanics*. Cambridge University Press. doi: <https://doi.org/10.1017/cbo9780511794780>
19. Aliev, T. I. (2009). *Osnovy modelirovaniya diskretnykh sistem*. Sankt-Peterburg, 363.
20. Iordanov, I. V., Simonova, Yu. I., Polozhy, A. V., Podkopayev, Ye. S., Skyrda, A. Ye., Kayun, A. P. (2020). A comprehensive study of the stability of lateral rocks with a supple support. *World Science*, 1 (1 (53)), 4–17. doi: [https://doi.org/10.31435/rsglobal\\_ws/31012020/6889](https://doi.org/10.31435/rsglobal_ws/31012020/6889)
21. Obiralov, A. I., Limonov, A. N., Gavrilova, L. A. (2006). *Fotogrammetriya i distantsionnoe zondirovaniye*. Moscow: Koloss, 335.
22. TSigler, F. (2002). *Mehanika tverdykh tel i zhidkostey*. Izhevsk, 912.
23. Akimov, V. A. et. al. (2010). *Teoreticheskaya mehanika. Dinamika. Praktikum. Chast' 2. Dinamika material'noy sistemy. Analiticheskaya mehanika*. Minsk: Novoe znanie; Moscow: TSUPL, 863.
24. Strelkov, S. P. (2005). *Vvedeniye v teoriyu kolebaniy*. Sankt-Peterburg: Lan', 440.
25. Gogo, V., Kipko, A., Vlasenko, N., Simonova, Y., Polozhy, A. (2019). Features of the stressed-deformed state of the side breeds in the assessment of the operational state of mining operations. *Journal of Donetsk Mining Institute*, 1, 53–64. doi: <https://doi.org/10.31474/1999-981x-2019-1-53-64>